

Electrochemical scanning tunneling microscopy analysis of the surface reactions on graphite basal plane in ethylene carbonate-based solvents and propylene carbonate

Minoru Inaba ^{*}, Zyun Siroma, Yutaka Kawatate, Atsushi Funabiki, Zempachi Ogumi

Department of Energy and Hydrocarbon Chemistry, Graduate School of Engineering, Kyoto University, Sakyo-ku, Kyoto 606-01, Japan

Accepted 14 September 1996

Abstract

In order to elucidate the mechanism of surface film formation on graphite negative electrodes of rechargeable lithium-ion batteries, topographical changes of the basal plane of a highly oriented pyrolytic graphite were observed in a few electrolyte solutions under polarization by electrochemical scanning tunneling microscopy. In 1 M LiClO₄/ethylene carbonate (EC) + diethyl carbonate, a hill-like structure of ~1 nm height appeared on the surface of highly oriented pyrolytic graphite at 0.95 V versus Li/Li⁺, and then changed at 0.75 V to irregular shaped blister-like features with a maximum height of ~20 nm. In 1 M LiClO₄/EC + dimethoxyethane, hemispherical blisters of ~20 nm height appeared at 0.90 V. These morphology changes, hill and blister formation, were attributed to the intercalation of solvated Li⁺ ions into graphite interlayers and to the accumulation of its decomposed products, respectively. On the other hand, only rapid exfoliation and rupturing of graphite layers were observed in 1 M LiClO₄/propylene carbonate (PC), which was considered to be responsible for ceaseless solvent decomposition when graphite electrodes are charged in PC-based solutions. From the observed topographical changes, it was concluded that the intercalation of solvated Li⁺ ions is a necessary step for stable surface film formation on graphite. © 1997 Elsevier Science S.A.

Keywords Secondary lithium batteries, Graphite negative electrodes, Solvent decomposition, Surface protective film, Scanning tunneling microscopy

1. Introduction

Graphite materials have been extensively studied for use as the negative electrodes in rechargeable lithium batteries [1–5]. It is generally accepted that the solvent decomposes to form a lithium-ion conductive surface film on graphite during the initial stage of charging [6–11]. The film suppresses further solvent decomposition, whereas lithium ions are intercalated through the surface film. The performance of graphite electrodes therefore should be affected by the nature of the surface film. Nevertheless, the mechanism of the film formation as well as its composition and morphology have not been fully clarified yet.

In previous studies [12,13], we observed topographical changes of highly oriented pyrolytic graphite (HOPG) basal plane in 1 M LiClO₄/ethylene carbonate (EC) + diethyl carbonate (DEC) by electrochemical scanning tunneling microscopy (STM) and elucidated the mechanism of surface film formation on graphite. When the sample potential was stepped to 1.1 V versus Li/Li⁺, a surface feature raised by

~1 nm with an atomically flat surface, which we call 'hill-like structure', appeared in the vicinity of a cleaving defect step, on the basal plane of HOPG. The hill spread out with time, and graphite layers on the hill slowly exfoliated. We attributed these topographical changes to the intercalation of solvated lithium ion, and inferred that this process is an initial step of surface film formation [13]. However, we could not observe STM images corresponding to subsequent processes of surface film formation because STM images became unclear at potentials more negative than 1.1 V under the previous experimental conditions. In this work, we present morphology changes taking place in EC-based solutions at potentials more negative than 1.1 V. In addition, morphology changes in propylene carbonate (PC) solution are examined for comparison.

2. Experimental

An electrochemical STM cell used for cyclic voltammetry and STM observation was described previously [13]. HOPG (Le Carbone Lorrain, PGCCL) was cleaved with an adhesive

^{*} Corresponding author; e-mail address: maba@sci.kyoto-u.ac.jp

tape to obtain a flat basal plane and used as the working electrode. Only the basal plane (0.20 cm^2) was brought into contact with the electrolyte solution. The electrolyte solution was 1 M LiClO_4 dissolved in EC+DEC (1:1 by volume), EC+dimethoxy ethane (DME) (1:1 by volume), or PC (Mitsubishi Chemical, Battery Grade). The counter and reference electrodes were platinum wire and lithium metal, respectively. Potential was measured and referred to as volts versus Li/Li^+ .

Electrochemical STM images were obtained with an SPI3600 system (Seiko Instruments) using an apiezone wax-coated Pt/Ir tip in the constant current mode. The potential of the tip electrode was fixed at 3.0 V. Initially the potential of the working electrode was kept at 2.8 V, where no reaction occurred. The potential was stepped to a lower potential for a given time, and then stepped back to 2.8 V, where STM images of the HOPG surface were obtained to visualize the surface reaction that occurred during the potential step. The step potential was successively lowered by 50 mV from 2.8 V. All measurements were carried out at room temperature in an argon-filled glove box.

3. Results and discussion

3.1. Cyclic voltammetry

Fig. 1 shows cyclic voltammograms at a scan rate of 5 mV s^{-1} of freshly cleaved HOPG basal plane in EC+DEC, EC+DME, and PC containing 1 M LiClO_4 . In each case several cathodic peaks appeared in the 0.5–1.0 V range on the first cathodic sweep, which are related to solvent decomposition and surface film formation processes. The number of cathodic peaks ranges from three to six depending on the kind of solvent, which implies that solvent decomposition and surface film formation processes are not a simple reaction. The first reduction peak rose at 1.0, 1.1, and 1.0 V in the EC+DEC, EC+DME, and PC solutions, respectively. The magnitude of the cathodic wave in EC+DME was larger than that in EC+DEC on the first cathodic sweep. While the cathodic peaks fully disappeared on the second sweep in

EC+DEC, the surface was not fully deactivated in EC+DME. This fact indicates that EC+DEC is more preferable for graphite electrodes than EC+DME with respect to stable passivating film formation. In the case of PC, a large reduction wave was observed even on the second sweep, which shows that protective film was not easily formed in PC. This result is consistent with the fact that solvent keeps decomposing at $\sim 1 \text{ V}$ when graphite electrodes are charged in PC-based solutions [14,15].

3.2. STM observation in EC-based solutions

The step potential was successively lowered by 50 mV from 2.8 V in 1 M $\text{LiClO}_4/\text{EC}+\text{DEC}$. The surface morphology remained unchanged at potentials more positive than 0.95 V. A typical image in this potential range is shown in Fig. 2(a), which was obtained after a potential step to 1.1 V for 1 min. The frame size of the image is $2 \mu\text{m} \times 2 \mu\text{m}$. Several cleaving defects, steps, running nearly parallel to one another were observed in this figure.

When the potential was stepped to 0.95 V, a morphology change was observed. Fig. 2(b) shows a surface morphology of nearly the same area as Fig. 2(a) after the potential was stepped to 0.95 V for 1 min. A hill-like structure of $\sim 1 \text{ nm}$ height appeared in the vicinity of a step edge in the upper left part of the image. The top surface of the hill was atomically flat. In our previous studies [12,13], we observed similar hills of $\sim 1 \text{ nm}$ height at 1.1 V in 1 M $\text{LiClO}_4/\text{EC}+\text{DEC}$. From the height change we concluded that the hill was formed by the intercalation of solvated lithium ions into graphite interlayers, which supported a solvent co-intercalation model for surface film formation that was proposed by Besenhard et al. [16]. The hill observed in Fig. 2(b) is considered to be the same kind of structure; however, it appeared at a potential somewhat lower than that in the previous studies [12,13]. In the previous studies, the morphology change with an elapse of time was observed keeping the electrode at a given potential in 1 M $\text{LiClO}_4/\text{EC}+\text{DEC}$, and the hill was formed at 1.1 V. The small current at 1.1 V in Fig. 1(a) implies that the kinetics of hill formation was very slow at this potential. Thus, the hill may not have appeared during a short reaction time of 1 min until 0.95 V in this study.

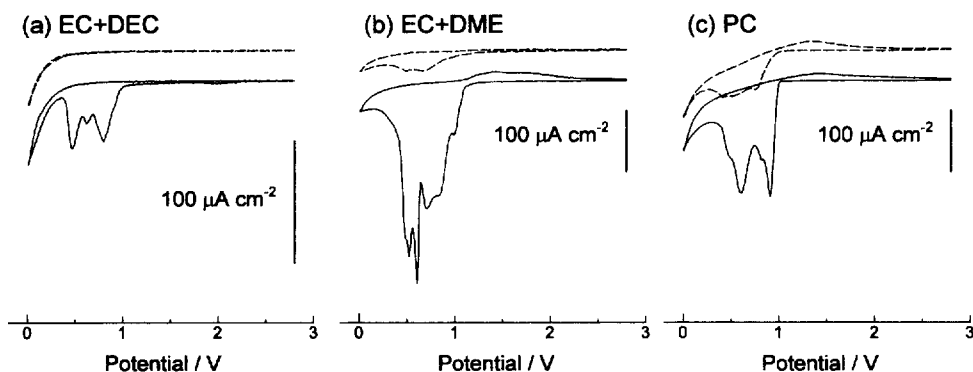


Fig. 1. Cyclic voltammograms of HOPG basal plane (0.20 cm^2) in 1 M LiClO_4 dissolved in: (a) EC+DEC (1:1 by volume); (b) EC+DME (1:1 by volume), and (c) PC; $v = 5 \text{ mV s}^{-1}$.

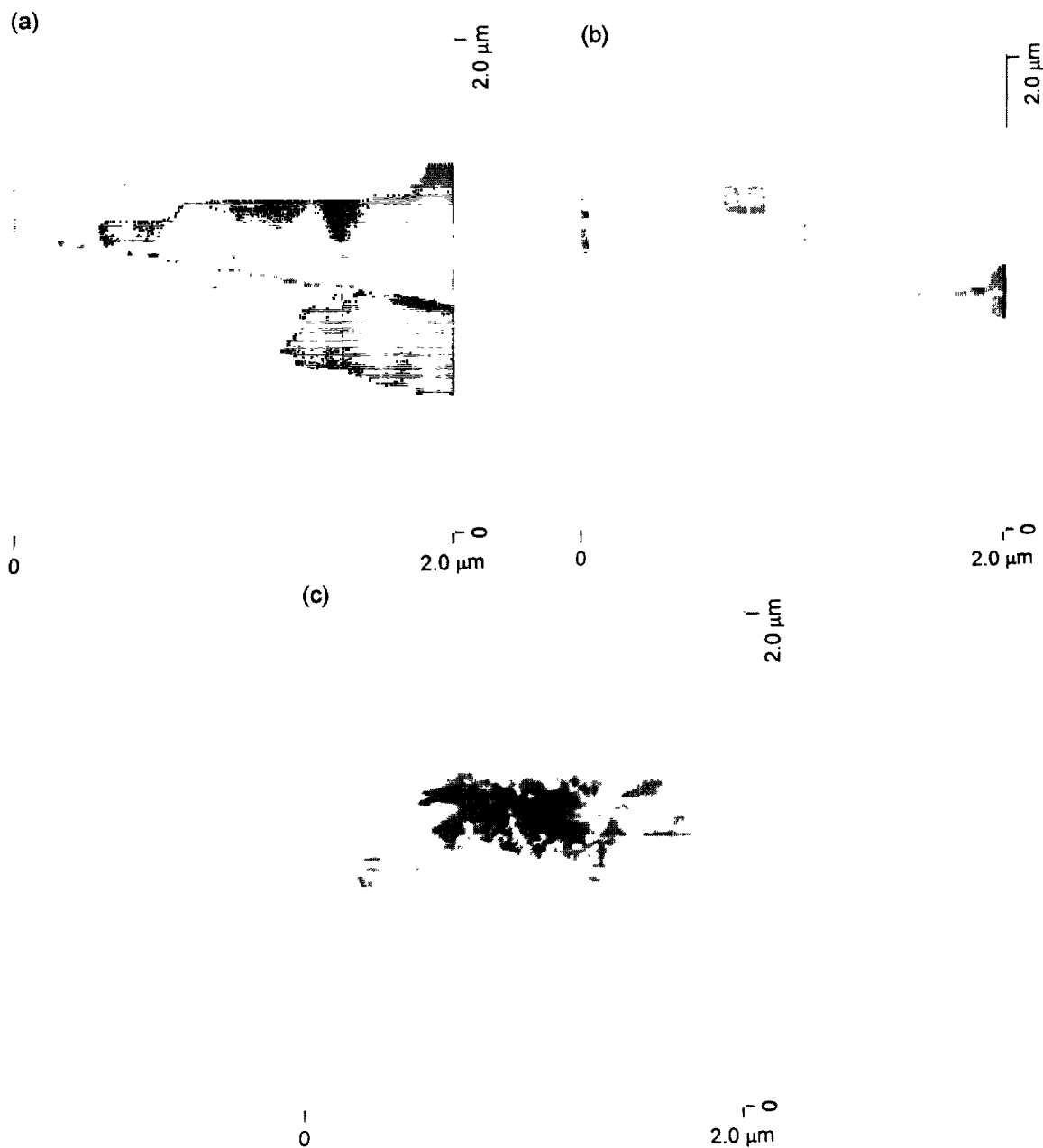


Fig. 2. STM images of HOPG basal plane surface after the potential was kept at: (a) 1.1; (b) 0.95, and (c) 0.75 V for 1 min in 1 M $\text{LiClO}_4/\text{EC} + \text{DEC}$. The frame size of each image is $2 \mu\text{m} \times 2 \mu\text{m}$.

An atomic scale STM image on the hill top was identical to that of the surrounding area. Both images showed every other atom of the individual carbon atoms as bright spots spaced by $\sim 0.25 \text{ nm}$, which are typical STM images of graphite basal plane [17,18]. This fact confirms that the hill was an interior structure formed under the surface. These images also suggested the AB stacking order of graphite layers just below the hill top, which shows that solvated Li^+ ions did not reside just below the top surface of the hill.

The solvent co-intercalation model states that the surface film is formed by the intercalation of solvated Li^+ ions followed by its decomposition to form an immobile product remaining between the graphite layers [16]. Topographical

changes corresponding to the decomposition process are expected to appear at more negative potentials, and hence the potential was further lowered. An image obtained after a potential step to 0.75 V for 1 min is shown in Fig. 2(c). The morphology was completely changed; irregular-shaped blister-like features appeared instead of the hill. The maximum height of the blisters was $\sim 20 \text{ nm}$, which was much larger than that of the hill ($\sim 1 \text{ nm}$) in Fig. 2(b). Although we cannot identify the origin of the blisters from the STM image, they seem to have been formed under the surface by accumulation of something or by gas evolution, which may be caused by the decomposition process of the solvated Li^+ ion according to the solvent co-intercalation model. At more neg-

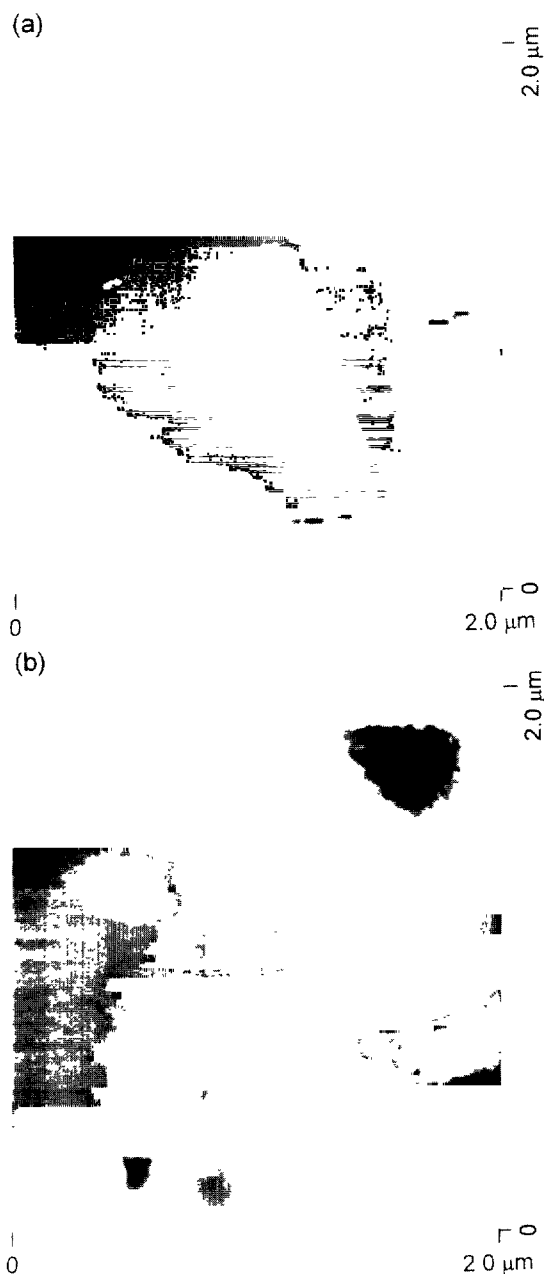


Fig. 3. STM images of HOPG basal plane surface obtained at 2.8 V after the potential was kept at (a) 1.1 and (b) 0.9 V for 3 min in 1 M LiClO₄/EC + DME. The frame size of each image is 2 μm × 2 μm.

ative potentials, the blisters are expected to grow to be a complete passivating layer; however, we could not obtain clear images at potentials more negative than 0.75 V, perhaps because of severe surface roughening or the formation of an electronically insulating surface layer.

The surface topographical change was observed in another EC-based solution, 1 M LiClO₄/EC + DME, in a similar manner. The surface morphology remained unchanged at potentials more positive than 1.0 V. Fig. 3(a) shows a typical STM image, which was obtained after the potential was stepped to 1.1 V for 3 min. Several steps were observed in this figure. After the potential was stepped to 0.9 V for 3 min,

a few hemispherical blisters appeared in the image (Fig. 3(b)). The lateral dimension and the maximum height of the blisters were 300–500 nm and ~20 nm, respectively. No hill formation was formed in this case. Although the shape of these blisters is different from that observed in EC + DEC, it is considered that they were also formed by the decomposition of the solvated Li⁺ ion. Close examination of the image revealed that step edges remained on the top surfaces of the blisters. This indicates that the blisters were interior structures formed by subsurface processes, which support our speculation that the blisters were formed under the surface by accumulation of decomposed products of the co-intercalated solvent or by gas evolution accompanied by decomposition.

3.3. STM observation in 1 M LiClO₄/PC

It is widely known that in a PC-based electrolyte solution, the solvent keeps decomposing at about 1.0 V and lithium is hardly intercalated into graphite [14,15]. Hence, solvent decomposition and surface film formation processes in PC-based solutions should greatly differ from those in EC-based solutions. Thus we observed the morphology change of the surface in a PC solution for comparison. The potential was successively lowered by 50 mV from 2.8 V in 1 M LiClO₄/PC. No morphology change was observed at potentials more positive than 0.95 V. Fig. 4(a) shows a typical image in this potential range, which was obtained after the potential was stepped to 1.1 V for 30 s. The frame size is 800 nm × 800 nm. Five terraces (A–E) separated four clear steps were observed in Fig. 4(a). After the potential was stepped to 0.95 V for 30 s (Fig. 4(b)), the lower part of terrace B was exfoliated and turned over to cover part of terrace A. The exfoliation proceeded further as the potential was lowered; however, neither hill nor blister formation was observed. Fig. 4(c) shows an image obtained after the potential was stepped to 0.7 V for 30 s. In Fig. 4(c), the surface became rough, indicating that graphite layers of the original terrace and step structure were ruptured significantly.

As shown in Fig. 4, neither hill-like structure nor blister was formed in 1 M LiClO₄/PC, and instead exfoliation and rupturing of graphite layers proceeded. In addition, the rate of exfoliation was much faster than that observed in the EC + DEC solution in the previous study [13]. Since the exfoliation was caused by some mechanical interlayer stress, it is reasonable to consider that graphite layers were exfoliated as soon as a solvated lithium ion intercalated into an interlayer. Whether hills and blisters are formed or not should therefore depend on the magnitude of interlayer stress caused by the intercalation of solvated Li⁺ ions, that is, to what extent the graphite host withstands the stress. When the stress is not so severe, solvated Li⁺ ions can stay securely between graphite layers and be subject to subsequent decomposition, resulting in stable passivating layer formation. Since the exfoliation of graphite layers leads to regeneration of highly reactive edge planes, the intercalation of solvated Li⁺ ions may

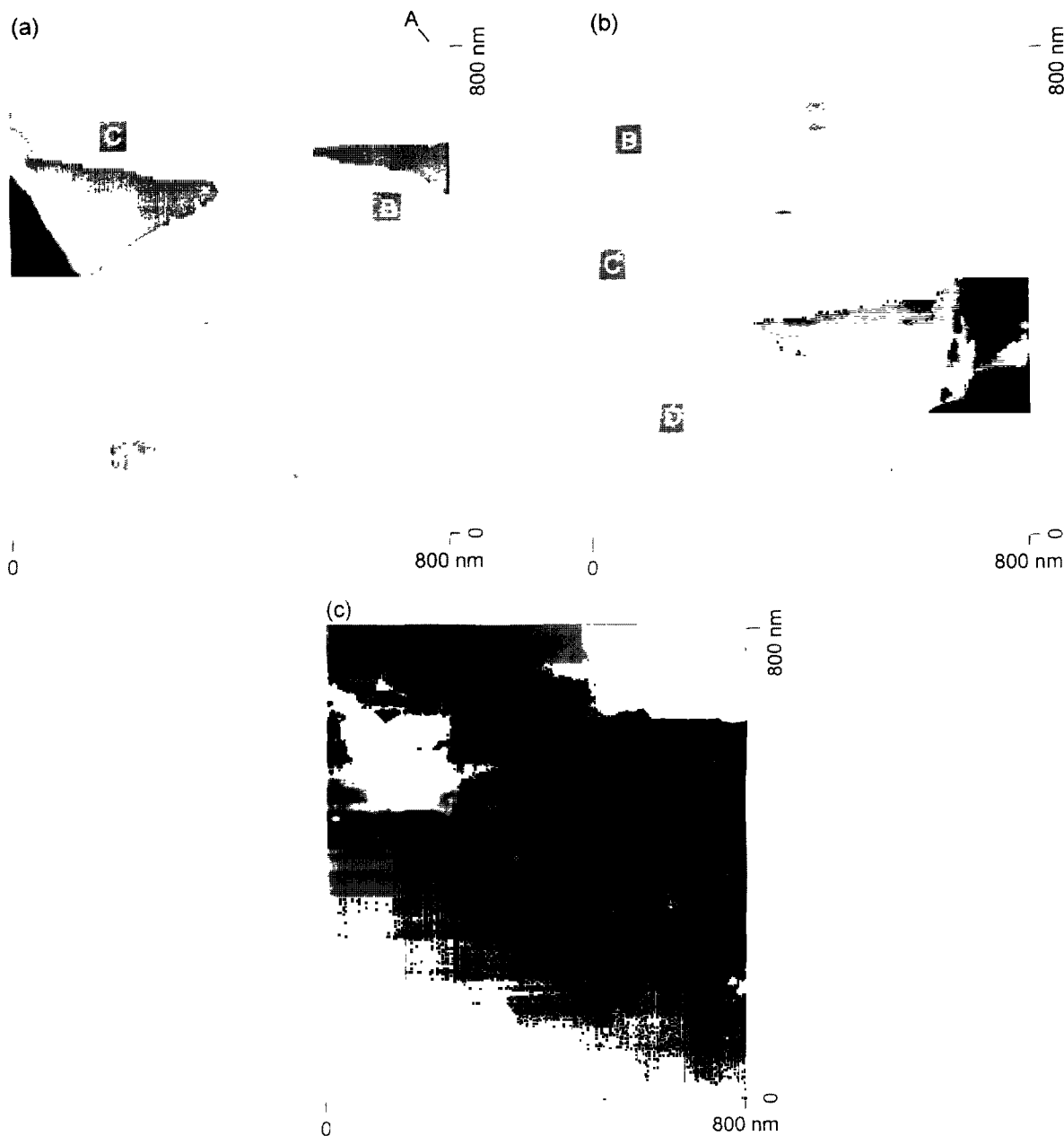


Fig. 4. STM images of HOPG basal plane surface after the potential was stepped to at (a) 1.1 V; (b) 0.95 V, and (c) 0.7 V for 30 s in 1 M LiClO₄/PC. The frame size of each image is 800 nm × 800 nm.

be an necessary step for stable surface film formation on graphite.

At the present stage, we do not know the reason why PC-solvated Li⁺ ions cause such a severe stress. Three possible origins may be inferred: the size of solvated Li⁺ ions, the electronic properties of resulting graphite intercalation compounds, and the chemical stability of the solvent itself. Further work is needed to clarify the stability of solvent-co-intercalated graphite host.

4. Conclusions

In situ electrochemical STM observation of the basal plane of HOPG in EC + DEC, EC + DME, and PC solutions con-

taining 1 M LiClO₄ was performed to clarify solvent decomposition and surface film formation processes. In the EC-based solutions, peculiar features, hills and blisters, appeared on the basal plane surface during the initial stage of charging. The observed morphology changes, hill and blister formation, were attributed to the intercalation of solvated Li⁺ ions into graphite interlayers and to the accumulation of its decomposed products, respectively, and supported the solvent co-intercalation model for surface film formation.

On the other hand, neither hill nor blister formation was observed in the PC solution, and instead rapid exfoliation and rupturing of graphite layers occurred. Since the exfoliation of graphite layers leads to regeneration of highly reactive

edge planes, stable protective film cannot be formed in such solutions. It was concluded that the intercalation of solvated Li^+ ions is a necessary step for stable surface film formation on graphite.

Acknowledgements

This work was partly supported by a Grant-in-Aid for Scientific Research (No. 07 455 426) from the Ministry of Education, Science and Culture, Japan and the Aid of Asahi Glass Foundation, Japan.

References

- [1] M. Mohri, N. Yanagisawa, Y. Tajima, H. Tanaka, T. Mitate, S. Nakajima, M. Yoshida, Y. Yoshida, Y. Yoshimoto, T. Suzuki and H. Wada, *J. Power Sources*, 26 (1989) 545.
- [2] J.R. Dahn, *Phys. Rev.*, B44 (1990) 9170.
- [3] N. Imanishi, H. Kashiwagi, T. Ichikawa, Y. Takeda, O. Yamamoto and M. Inagaki, *J. Electrochem. Soc.*, 140 (1993) 315.
- [4] R. Yazami and D. Guerard, *J. Power Sources*, 43–44 (1993) 39.
- [5] M. Inaba, H. Yoshida, Z. Ogumi, T. Abe, Y. Mizutani and M. Asano, *J. Electrochem. Soc.*, 142 (1995) 20.
- [6] R. Fong, U. von Sacken and J.R. Dahn, *J. Electrochem. Soc.*, 137 (1990) 2009.
- [7] Z.X. Shu, R.S. McMillan and J.J. Murray, *J. Electrochem. Soc.*, 140 (1993) L101.
- [8] Z.X. Shu, R.S. McMillan and J.J. Murray, *J. Electrochem. Soc.*, 140 (1993) 922.
- [9] M. Ishikawa, M. Morita, M. Asano and Y. Matsuda, *J. Electrochem. Soc.*, 141 (1994) 1105.
- [10] D. Aurbach, Y. Ein-Eli, O. Chusid, Y. Carmeli, M. Babai and H. Yamin, *J. Electrochem. Soc.*, 141 (1994) 603.
- [11] T. Ein-Eli, B. Markovsky, D. Aurbach, Y. Carmel, H. Yamin and S. Luski, *Electrochim. Acta*, 29 (1994) 2559.
- [12] M. Inaba, Z. Siroma, Z. Ogumi, T. Abe, Y. Mizutani and M. Asano, *Chem. Lett.*, 661 (1995).
- [13] M. Inaba, Z. Siroma, A. Funabiki, Z. Ogumi, T. Abe, Y. Mizutani and M. Asano, *Langmuir*, 12 (1996) 1535.
- [14] A.N. Dey and B.P. Sullivan, *J. Electrochem. Soc.*, 117 (1970) 220.
- [15] M. Arakawa and J. Yamaki, *J. Electroanal. Chem. Interfacial Electrochem.*, 219 (1987) 273.
- [16] J.O. Besenhard, M. Winter, J. Yang and W. Biberacher, *J. Power Sources*, 54 (1995) 228.
- [17] S. Morita, S. Tsukada and J. Mikoshiba, *J. Vac. Sci. Technol.*, A6 (1988) 354.
- [18] D. Tománek and S.G. Louie, *Phys. Rev.*, B37 (1988) 9327.